

520 **Supplementary Materials for**

521 **Multimodal identification of rare potent effector CD8 T cells in solid tumors**

522 Arja Ray^{1,2}, Molly Bassette^{1,2}, Kenneth H. Hu^{1,2,#}, Lomax F. Pass^{1,2}, Bushra Samad^{2,3},
523 Alexis Combes^{1,2,3,5}, Vrinda Johri^{2,3}, Brittany Davidson^{2,3}, Grace Hernandez⁴, Itzia Zaleta-
524 Linares^{1,2}, Matthew F. Krummel^{1,2*}

525

526

527 **Affiliations:**

528 ¹Department of Pathology, ²ImmunoX Initiative, ³UCSF CoLabs, ⁴Department of
529 Anatomy, ⁵Department of Medicine, University of California, San Francisco, CA 94143,
530 USA. # Current Address: Department of Immunology, The University of Texas MD
531 Anderson Cancer Center and James P Allison Institute

532

533

534

535 ***Corresponding Author:**

536 Matthew F. Krummel, Ph.D.

537 513 Parnassus Avenue, HSW 512

538 San Francisco, CA 94143-0511

539 matthew.krummel@ucsf.edu

540 Tel: (415) 514-3130

541 Fax: (415) 514-3165

542

543

544

545

546

547

548

549

550

551

552 **Materials and Methods**

553 **Mice:** All mice were treated in accordance with the regulatory standards of the National Institutes
554 of Health and American Association of Laboratory Animal Care and were approved by the UCSF
555 Institution of Animal Care and Use Committee. Cd69-TFP-CreER^{T2} (denoted as Cd69-TFP) mice
556 in the C57BL6/J background were custom-generated from Biocytogen Inc. and then maintained
557 heterozygous (bred to C57BL6/J wild type mice) at the UCSF Animal Barrier facility under specific
558 pathogen-free conditions. C57BL6/J (wild type; WT), C57BL6/J CD45.1 (B6.SJL-Ptprc^a
559 Pepc^b/BoyJ), OT-I (C57BL/6-Tg(TcraTcrb)1100Mjb/J) mice were purchased for use from Jackson
560 Laboratories and maintained in the same facility in the C57BL6/J background. For adoptive
561 transfer experiments, CD45.1^{het}; OT-I^{het}; Cd69-TFP^{het} (denoted simply as CD45.1; OT1; Cd69-
562 TFP) mice were used. Mice of either sex ranging in age from 6 to 14 weeks were used for
563 experimentation. For experiments using the transgenic PyMTchOVA strain(21), mammary tumor-
564 bearing females in the age range of 15 to 24 weeks were used. Adoptive transfer of T cells in
565 these mice were done when mice developed at least 2 palpable tumors (> 25-30mm²).

566 **Mouse tumor digestion and flow cytometry:** Tumors from mice were processed to generate
567 single cell suspensions as described previously(34). Briefly, tumors were isolated and
568 mechanically minced on ice using razor blades, followed by enzymatic digestion with 200 µg/mL
569 DNase (Sigma-Aldrich), 100U/mL Collagenase I (Worthington Biochemical) and 500U/mL
570 Collagenase IV (Worthington Biochemical) for 30 min at 37°C while shaking. Digestion was
571 quenched by adding excess 1X PBS, filtered through a 100µm mesh, spun down and red blood
572 cells were removed by incubating with RBC lysis buffer (155 mM NH₄Cl, 12 mM NaHCO₃, 0.1 mM
573 EDTA) at room temperature for 10 mins. The lysis was quenched with excess 1X PBS, spun down
574 and resuspended in FACS buffer (2mM EDTA + 1% FCS in 1X PBS) to obtain single cell
575 suspensions. Similarly, tumor draining lymph nodes (dLN) were isolated and mashed over 100µm
576 filters in PBS to generate single cell suspensions.

577 For each sample, 2.5-3 million cells/sample were stained in a total of 50 μ L of antibody mixture for
578 flow cytometry. Cells were washed with PBS prior to staining with Zombie NIR Fixable live/dead
579 dye (1:500) (Biolegend) for 20 min at 4°C. Cells were washed in FACS buffer followed by surface
580 staining for 30 min at 4°C with directly conjugated antibodies diluted in FACS buffer containing
581 1:100 anti-CD16/32 (Fc block; BioXCell) to block non-specific binding. Antibody dilutions ranged
582 from 1:100-1:400, optimized separately. After surface staining, cells were washed again with
583 FACS buffer. For intracellular staining, cells were fixed for 20 min at 4°C using the IC Fixation
584 Buffer (BD Biosciences) and washed in permeabilization buffer from the FoxP3 Fix/Perm Kit (BD
585 Biosciences). Antibodies against intracellular targets were diluted in permeabilization buffer
586 containing 1:100 Fc Block and cells were incubated for 30 min at 4°C followed by another wash
587 prior to readout on a BD LSRII or Fortessa Cytometer.

588 **Processing and flow cytometry analysis of other mouse organs:** To phenotype T cells under
589 from lymphoid organs homeostasis, spleen and inguinal, mesenteric and brachial lymph nodes
590 were isolated and mashed over 100 μ m filters washed with 1X PBS to generate single cell
591 suspension of lymphocytes. For splenic suspensions, RBC lysis was performed as described
592 above before staining for flow cytometry.

593 To profile thymocytes, thymus was isolated, cut into small pieces with a razor blade and minced
594 by using gentleMACS dissociator (Miltenyi Biotec) in RPMI. Next, the mixture was spun down and
595 resuspended in the digestion mixture described above and allowed to digest with shaking at 37°C
596 for 20 mins, following which, the remaining tissue was either minced again using the gentleMACS
597 dissociator and/or directly mashed over a 100 μ m filter in FACS buffer to generate a single cell
598 suspension, ready to be processed for staining and flow cytometry.

599 Skin digestion was done as previously described(35). Briefly, mice are shaved and depilated prior
600 to removal of dorsal skin. The skin was then rid of fat, minced with scissors and razor blade in the
601 presence of 1 ml of digest media (2 mg/ml collagenase IV (Roche), 1 mg/ml hyaluronidase

602 (Worthington), 0.1 mg/ml DNase I (Roche) in RPMI-1640 (GIBCO). The minced skin was then
603 moved to a 50 ml conical with 5 ml additional digest solution and incubated at 37°C for 45 min
604 with shaking and intermittent vortexing before being washed and passed through a 70µm strainer
605 prior to staining. TFP high vs. low gates were drawn by using a side-by-side WT control or using
606 endogenous CD8 T cells in the context of adoptive transfer into a tumor-bearing mouse.

607 **Tumor injections and adoptive transfer of CD8 T cells into tumors:** The B78chOVA and
608 MC38chOVA cancer cell lines, as previously described(14, 34), were generated by incorporating
609 the same mcherry-OVA construct used to establish the PyMTchOVA spontaneous mouse
610 line(21). For tumor injections, the corresponding cells were grown to near confluency (cultured in
611 DMEM with 10% FCS (Benchmark) and 1% PSG (Gibco)) and harvested using 0.05% Trypsin-
612 EDTA (Gibco) and washed 3x with PBS (Gibco). The number of cells to be injected per mouse
613 was resuspended in PBS and mixed in a 1:1 ratio with Growth Factor Reduced Matrigel (Corning)
614 to a final volume of 50µL per injection. The mixture was injected subcutaneously into the flanks
615 of anesthetized and shaved mice. Tumors were allowed to grow for 14–21 days unless otherwise
616 noted, before tumors and tumor-draining lymph nodes were harvested for analysis. CD8 T cells
617 were isolated from CD45.1;OT-1;Cd69-TFP mice using the EasySep Negative Selection Kit (Stem
618 Cell Bio), resuspended in 1X PBS at 10X concentration 100µL was injected into each tumor-
619 bearing mice. For B78chOVA and PyMTchOVA tumors, 1 million and for MC38chOVA tumors,
620 200,000 CD8 T cells were injected retro-orbitally into each mouse either 5d (B78chOVA), 7d
621 (MC38chOVA) post tumor injection or when mice had at least 2 palpable tumors (PyMTchOVA).
622 Tumor measurements were done by measuring the longest dimension (length) and approximately
623 perpendicular dimension (width) using digital calipers, rounded to one decimal place each.

624 **Contralateral tumor injection and vaccination:** 5 days post B78chOVA tumor injection, equal
625 numbers (1 million) CD8 T cells from a CD45.1;OT-1;Cd69TFP and P14;Cd69TFP mice were
626 injected retroorbitally into each mice. Next day, gp33-41 subcutaneous peptide (Anaspec)

627 vaccination was injected contralaterally to the tumor, with 50 μ g peptide + 50 μ L Common Freund's
628 Adjuvant (CFA, Sigma) along with 50 μ L PBS for a total volume of 100 μ L. The vaccination site
629 was identified by a white, hardened subcutaneous mass and isolated and processed similarly to
630 the tumor for flow cytometry.

631 **In vitro stimulation of naïve CD8 T cells:** CD8 T cells were isolated from Cd69-TFP or WT mice
632 as described above and plated in a 96 well round bottom plate (Corning) at 80,000 cells/well in T
633 cell media-RPMI (Gibco) + 10% FCS (Benchmark) + Penicillin/Streptomycin + Glutamine (Gibco).
634 TCR stimulation was induced by adding anti-CD3/CD28 Dynabeads (Applied Biosystems) at the
635 concentration of 2 μ L per 80,000 cells (1:1 ratio of cells:beads), the plate was briefly spun down
636 to bring cells and beads together before incubation at 37°C for varying lengths of time. 55 μ M β -
637 mercaptoethanol (BME; Gibco) was added to the T cell media during stimulation. For repeated
638 stimulation assays, 2 wells of each sample at every time point were pooled for mRNA isolation
639 and qRT-PCR, while 2 other wells were used as duplicates for flow cytometry. After each cycle,
640 beads taken off each well and replated for resting in T cell media containing 10 U/mL of
641 Interleukin-2 (IL-2; Peprotech). To restart each stimulation cycle, cells from each biological
642 replicate were pooled, counted and Dynabeads were added at the appropriate concentration for
643 a 1:1 ratio and redistributed into wells for incubation.

644 **Sorting and qPCR, resting or restimulation of homeostatic CD8 T cells:** To sort sufficient
645 CD8 T cells from homeostatic lymphoid organs, CD8 T cells were first isolated from spleens and
646 inguinal, brachial, mesenteric lymph nodes Cd69-TFP or WT mice using the EasySep Negative
647 selection kit. These cells were then sorted on TFP^{hi} (top 15%), TFP^{mid} (middle 30%) and TFP^{lo}
648 (bottom 15%) from each mouse separately and rested in T cell media containing 10 U/mL
649 Interleukin-7 in a 96 well round bottom plate and assayed at 0, 24 and 48h. Likewise, for qPCR
650 analysis of populations high, mid and low for TFP, these populations were sorted into cold T cell
651 media, pelleted and subjected to RNA extraction and qPCR with primers for Cd69 and 18s rRNA

652 as the reference gene. For the sort and restimulation experiment, Memory (CD44+CD62L+) TFP^{hi}
653 cells and Effector (CD44+CD62L-) TFP^{lo} cells were sorted and incubated in T cell media + 55µM
654 BME containing 1:1 anti CD3/CD28 Dynabeads in a 96 well round bottom plate with either 5µg/mL
655 Actinomycin D (Sigma) in DMSO or DMSO alone (vehicle) for 3h, before profiling by flow
656 cytometry. De novo CD69 surface expression was measured by the difference of CD69 MFI
657 between the vehicle and Actinomycin D treated groups.

658 **Restimulation and cytokine production of intratumoral CD8 T cells:** OT-I T cells from
659 B78chOVA tumors were sorted on a BD FACSAria Fusion or BD FACSAria2 (BD Biosciences) at
660 d11-d13 post adoptive transfer of CD8 T cells from CD45.1; OT-I; Cd69-TFP mice, as described
661 above. To prepare CD45-enriched fractions(36), tumors were digested as described above into
662 single cell suspensions, centrifuged and resuspended in 30mL room temperature (RT) RPMI
663 1640. Then, 10mL Ficoll-Premium 1.084 (Cytiva) was carefully underlaid and the tubes
664 centrifuged at 1025g for 20 mins at RT without braking. The resulting interface-localized cells
665 were pipetted out, diluted in equal volume RPMI and centrifuged at 650g for 5 mins to collect the
666 cells. This constituted a CD45-enriched fraction which was then processed for staining and FACS.
667 The four CD69:TFP quadrants were sorted from each tumor sample (cells from 2-3 tumor samples
668 were pooled for a single biological replicate) into serum-coated microcentrifuge tubes containing
669 cold T cell media. These were subsequently plated in a 96-well V-bottom plate either in T cell
670 media or T cell media containing PMA (50 ng/mL; Sigma-Aldrich), Ionomycin (500ng/mL;
671 Invitrogen) + Brefeldin A (3µg/mL; Sigma-Aldrich) and BME (Gibco) for 3h, before cells were
672 collected for surface and intracellular staining for cytokines and granzyme B.

673 **Long-term ex vivo tumor slice overlay:** Tumor slice overlay cultures were adapted, modified
674 and extended from previous work(22). For tumor slice overlay cultures, B78chOVA tumors were
675 injected bilateral subcutaneously into the flank of anesthetized and shaved mice. Tumors were
676 allowed to grow for 11 – 13 days. 96 hours prior to tumor harvest and slicing, CD8 T cells were

677 isolated from CD45.1;OT-1;Cd69-TFP mice, as described above. Isolated CD8 T cells were
678 activated via 1:1 culture with Dynabeads Mouse T-Activator CD3/CD28 (Invitrogen) in T cell
679 media + BME in 96 well U-bottom plates for 48 hours. After activation, T cells were removed from
680 Dynabeads rested in T cell media with supplemented 10 U/mL IL-2 (PeproTech) for 48 hours
681 before use. For gating TFP high vs. low cells, CD8 T cells from CD45.1; OT-I mice were subjected
682 to similar pre-treatment and profiled by flow cytometry side-by-side along with the CD45.1;OT-
683 1;Cd69-TFP CD8 T cells at d0.

684 For slicing, tumors were harvested and stored in cold RPMI until use. Each well of a 24 well plate
685 was pre-filled with cold RPMI and stored on ice. Tumors were embedded in 1.5-2% agarose gel,
686 allowed to solidify, and sliced at a thickness of 350 – 400 μ m using a Compressstome VF310-0Z
687 Vibrating Microtome (Precisionary). Slices were immediately stored in pre-filled 24 well plate on
688 ice until use.

689 For the slice overlay, each well of a 24 well plate was pre-coated with 30 μ L of 1 part culture
690 medium:4 parts Matrigel and allowed to solidify at 37°C. Tumor slices were removed from RPMI
691 and excess agarose was trimmed from slice edges (leaving a thin halo of agarose around slices
692 to use for handling). Slices were spread across solidified Matrigel bed in 24 well plates. Rested T
693 cells were stained with Violet Proliferation Dye 450 (BD Biosciences) diluted 1:1000 in PBS at 10
694 x 10⁶ cells/mL for 15 minutes at 37°C. Cells were washed 2x with PBS and resuspended in T cell
695 culture medium at 150 – 200 x 10⁶ cells/mL. 5 μ L cell suspension (0.5 – 1 x 10⁶ cells) was added
696 directly on top of each slice and incubated at 37°C for 3 hours, with 5 μ L fresh media added to
697 each slice every 30 minutes to prevent slices from drying out. After incubation, 30 μ L non-diluted
698 Matrigel was added directly atop each slice and allowed to solidify at 37°C. 2mL T cell culture
699 medium containing BME was added to each well. 1mL culture medium was removed and replaced
700 with fresh medium every 24 hours throughout the experiment.

701 **Single cell RNA Sequencing and Analysis:** Adoptively transferred CD45.1; OT-I; Cd69-TFP
702 CD8 T cells were sorted from B78chOVA tumors d12 post transfer into four populations based on
703 the CD69:TFP quadrants (Q1: TFP+/CD69-, Q2: TFP+/CD69+, Q3: TFP-/CD69-, and Q4: TFP-
704 /CD69+). Sorted cells were separately labeled with lipid and cholesterol-modified oligonucleotides
705 (LMO's) according to McGinnis et. al(37). Following 2 washes with PBS + 0.1% BSA, cells were
706 pooled for encapsulation in one lane of a 10X 3' v3 kit with a target cell number of 18,000.

707 Following construction of the GEX library (according to manufacturer's instructions) and the LMO
708 library(37), libraries were pooled at a 10:1 molar ratio for sequencing on the NovaSeq 6000. This
709 resulted in 807M cDNA reads and 163M LMO reads. Transcript and LMO reads were counted
710 using the CellRanger count function against the GRCm38 reference genome to generate feature
711 barcode matrices. These matrices were loaded into Seurat and filtered to remove high
712 mitochondrial % cells (> 15%) and cells with low nGene (< 200 genes). Cells were then
713 demultiplexed using their LMO counts with cells having too few LMO nUMI or ambiguous identity
714 (possible multiplets) filtered out using the demultiplex package(37). The resulting object had an
715 average cDNA nUMI per cell of 7662 reads and average nGene per cell of 2115 genes and
716 average LMO nUMI per cell of 1080 reads. The final object underwent scaling and then scoring
717 for cell cycle signatures (S and G2M scores as computed using Seurat's built-in CellCycleScoring
718 function. The object then underwent regression for cell cycle effects (S and G2M score as
719 described in the Seurat vignette) and percent mitochondrial reads before PCA. K-Means
720 clustering and UMAP dimensional reduction was then performed on the first 16 PC's.

721 Established subpopulations of exhausted T cells were marked by expression of canonical genes
722 such as Stem-like or Progenitor (T_{EX}^{Prog} ; *Tcf7*, *Ccr7*, *Jun*) (8, 12), Early Effector-like ($T_{EX}^{E.Eff}$;
723 *Hsp90aa1*, *Hsp90ab1*, *Npm1*) (38), Late Effector or KLR-gene-expressing effector-like ($T_{EX}^{KLR.Eff}$;
724 *Klrd1*, *Zeb2*) (8), Memory T_{EX}^{Mem} . (*Cxcr3*, *Ly6c2*, *Itgb7*) (39) and Interferon-Stimulated T_{EX}^{ISG}
725 (*Cxcl10*, *Isg15*, *Ifit1*) (**Fig. S8A**). The Intermediate ($T_{EX}^{Int.}$) and Terminal ($T_{EX}^{Term.}$) subsets were

726 distinguished by exhaustion-related genes *Ctla4*, *Pdcd1*, *Tox* and those related to actin
727 organization and TCR signaling such as *Tmsb4x*, *Coro1a*, *Actg1*, *Ccl5* and *S100a6*(8).
728 Additionally, two cell cycle gene-dominated clusters termed T_{EX}^{Cyc1} T_{EX}^{Cyc2} were identified (**Fig.**
729 **3B, Fig. S8A**).

730 Cytotoxic and exhaustion scores were generated by calculating the average expression of
731 ensemble gene lists for each of the phenotypes—Exhaustion: *Ctla4*, *Pdcd1*, *Cd38*, *Entpd1*, *Tox*;
732 Cytotoxic: *Prf1*, *Gzmc*, *Tnfrsf9*, *Ifng*, *Klrd1*.

733 **qRT-PCR:** At designated time points, CD8 T cells were isolated from the 96 well culture plates,
734 or CD8 T cells were sorted into T cell media and centrifuged. The supernatant was aspirated out
735 and the pellets stored at -80°C until mRNA extraction using the RNEasy Micro Kit (Qiagen).
736 Corresponding cDNA was synthesized from the mRNA samples using the cDNA amplification kit
737 (Applied Biosystems). qPCR using pre-designed *Cd69* and *18s* probes (Invitrogen) with a
738 TaqMan-based assay system (BioRad) or custom-made primers (iDT Technologies) for *Jun* (Fwd:
739 5' ACGACCTTCTACGACGATGC 3', Rev: 5' CCAGGTTCAAGGTCATGCTC 3')(40) , *Stat5a*
740 (Fwd: 5' CGCTGGACTCCATGCTTCTC 3', Rev: 5' GACGTGGGCTCCTTACTACTGA 3')(41) and
741 *18s* (Fwd: 5' CTTAGAGGGACAAGTGGCG 3', Rev: 5' ACGCTGAGCCAGTCAGTGTA 3')(42)
742 using the SsoFast assay system (BioRad) was used to quantify transcripts in a BioRad CFX94
743 machine.

744 **Human tumor samples:** All tumor samples were collected with patient consent after surgical
745 resection under a UCSF IRB approved protocol (UCSF IRB# 20-31740), as described
746 previously(29). In brief, freshly resected samples transported in ice-cold DPBS or Leibovitz's L-
747 15 medium before digestion and processing to generate a single-cell suspension. The following
748 cancer indications were included in the cohort: Bladder cancer (BLAD), colorectal cancer (CRC),
749 glioblastoma multiforme (GBM), gynecological cancers (GYN), hepatocellular cancers (HEP),
750 head and neck cancer (HNSC), kidney cancer (KID), lung cancer (LUNG), melanoma (MEL),

751 pancreatic ductal adenocarcinoma (PDAC), pancreatic neuroendocrine tumors (PNET), sarcoma
752 (SRC).

753

754 **Transcriptomic analysis of human tumors:** All tumor samples were collected under the UCSF
755 Immunoprofiler project as described(29). Briefly, tumor samples were thoroughly minced with
756 surgical scissors and transferred to GentleMACs C Tubes containing 800 U/ml Collagenase IV
757 and 0.1 mg/ml DNase I in L-15/2% FCS per 0.3 g tissue. GentleMACs C Tubes were then installed
758 onto the GentleMACs Octo Dissociator (Miltenyi Biotec) and incubated for 20 min (lymph node)
759 or 35 min (tumor) according to the manufacturer's instructions. Samples were then quenched with
760 15 mL of sort buffer (PBS/2% FCS/2mM EDTA), filtered through 100µm filters and spun down.
761 Red blood cell lysis was performed with 175 mM ammonium chloride, if needed. Freshly digested
762 tumor samples were sorted by FACS into conventional T cell, Treg, Myeloid, tumor and in some
763 cases, stromal compartments and bulk RNA-seq was performed on sorted cell fractions. mRNA
764 was isolated from sorted fractions and libraries were prepared using Illumina Nextera XT DNA
765 Library Prep kit. The libraries were sequenced using 100bp paired end sequencing on HiSeq4000.
766 The sequencing reads we aligned to the Ensembl GRCh38.85 transcriptome build using
767 STAR(43) and gene expression was computed using RSEM(44). Sequencing quality was
768 evaluated by in-house the EHK score, where each sample was assigned a score of 0 through 10
769 based on the number of EHK genes that were expressed above a precalculated minimum
770 threshold. The threshold was learned from our data by examining the expression distributions of
771 EHK genes and validated using the corresponding distributions in TCGA. A score of 10
772 represented the highest quality data where 10 out of 10 EHK genes are expressed above the
773 minimum threshold. The samples used for survival analysis and other gene expression analyses
774 had an EHK score of greater than 7 to ensure data quality. Ensemble gene signatures scores

775 were calculated by converting the expression of each gene in the signature to a percentile rank
776 among all genes and then determining the mean rank of all the genes in the signature.

777

778 **Reanalysis of published datasets:** Available, curated RNA-Seq data (5, 7, 14) on *Cd69* and
779 upstream transcription factor expression was plotted directly without modification. A curated R
780 object derived from Zheng et al.(30) generously shared by Dr. Miguel Reina-Campos, UCSD, was
781 used for analysis in Fig. 5. Ensemble gene signatures were scored as mentioned above and
782 plotted onto pre-existing UMAP dimensional reduction and already annotated cell clusters. While
783 exhaustion and T*_{EFF} genes were obtained from previously published work (29) and this study
784 respectively, *TCF7*, *SELL*, *LEF1*, *CCR7*, *IL7R* genes were used for the Naïve score.

785

786 **In vitro Killing Assay:** MC38chOVA tumors with adoptively transferred Cd69-TFP-OT-I CD8 T
787 cells in WT B6 mice were harvested at d8 post T cell transfer, digested as mentioned above, and
788 sorted by CD69: TFP quadrants into cold T cell media. Sorted cells were centrifuged,
789 resuspended in fresh, warm T cell media with BME and added onto MC38chOVA cells plated
790 ~24h prior in flat-bottom 96 well plates. To each well containing 5000 MC38chOVA plated 24h
791 prior, 5000 sorted T cells were added. As with the sort and restimulation experiments, each such
792 collection of 5000 cells from a particular quadrant was pooled from 2-3 tumors and treated as a
793 single biological replicate. Each experiment involved 7-8 tumors to obtain at least 3 biological
794 replicates. Technical replicates were included and averaged wherever possible, i.e., at least
795 10,000 cells were sorted from a given quadrant and biological replicate. Percentage killing was
796 obtained by measuring the fractional loss of live cells at 36h in no T cell vs. T cell added conditions
797 relative to 0h. Live cell numbers from each condition was accurately measured by lightly detaching

798 cancer cells with trypsin and scoring against CountBright (ThermoFisher) absolute counting
799 beads on a flow cytometer.

800

801 **CITE-Seq analysis of human tumors:** For CITE-Seq, post tumor digestion, cells were incubated
802 with Human TruStain FcX Receptor Blocking Solution to prevent non-specific antibody binding
803 before staining with Zombie Aqua Fixable Viability Dye and anti-human CD45 antibody in
804 PBS/2%FCS/2mM EDTA/0.01% sodium azide and incubated for 25 min on ice in the dark. Live
805 CD45⁺ and CD45⁻ cells were sorted on a BD FACSAria Fusion. CD45⁺ and CD45⁻ cells were
806 pelleted and resuspended at 1x10³ cells/ml in 0.04%BSA/PBS buffer before mixing in an 8:2
807 CD45⁺:CD45⁻ ratio and loaded onto the Chromium Controller (10X Genomics) to generate 5' v1.1
808 gel beads-in-emulsions (GEM). Pooled 8:2 CD45⁺:CD45⁻ cells were resuspended in
809 Cell Staining Buffer (BioLegend) and stained with a pool of 137 TotalSeq-C antibodies (Table)
810 according to the manufacturer's protocol before loading onto the Chromium Controller (10X
811 Genomics) for GEM generation. The cDNA libraries were generated using all or a subset of
812 Chromium Next GEM Single Cell 5' Library Kit for gene expression (GEX), Chromium Single Cell
813 V(D)J Enrichment kit (10X Genomics) for T cell receptor (TCR), and Chromium Single Cell 5'
814 Feature Barcode Library kit for antibody derived tag (ADT) according to the manufacturer's
815 instructions. The libraries were subsequently sequenced on a Novaseq S4 sequencer (Illumina)
816 to generate fastqs with the following mean reads per cell: 42,000 (GEX), 34,000 (TCR), and 5,700
817 (ADT). For multimodal clustering and analysis, CLR normalization followed by weighted nearest
818 neighbor (WNN) clustering was performed using the Seurat package in R. Naïve and Exhaustion
819 scores were generated using the percentile rank method as mentioned above, but with protein
820 (ADT) markers- Naïve : CD62L, CD45RA, IL7RA; Exhaustion: PD-1, CTLA-4, CD38, CD39.

821

822 **Live 2-photon imaging of tumor slices and image analysis:** Live imaging of tumor slices was
823 performed on a custom-made 2-photon microscope as previously described(1). Briefly, 1 million
824 CD2dsRed; OT-I; Cd69-TFP or control CD2dsRed; OT-I CD8 T cells were retro-orbitally injected
825 into WT mice bearing MC38chOVA tumors injected 5-7d earlier and harvested 7-10d after T cell
826 injection. Slices for imaging were generated as described above for the ex vivo slice culture assay.
827 Slices were placed in a custom-made perfusion chamber and imaged under oxygenated and
828 temperature-controlled perfusion of RPMI 1640, as described previously(1). Dual laser excitations
829 at 825nm and 920nm were used to excite the requisite fluorophores. Image analysis was
830 performed on Imaris (BitPlane) with custom-made plugins developed on Matlab (Mathworks) and
831 Fiji. Surfaces were generated on CD8 T cells and in both CD2dsRed; OT-I and CD2dsRed; OT-
832 I; Cd69-TFP bearing slices and the corresponding levels of the former in the 515-545nm range
833 PMT were used to gate on TFP^{hi} vs. TFP^{lo} OT-I.

834 Cell tracking was performed on Imaris and corresponding cell positions imported to Matlab for
835 further analysis to fit the persistent random walk model (PRWM) to the cell trajectories(45) using
836 the method of overlapping intervals (46). Briefly, the mean squared displacement (MSD) for a cell
837 for given time interval t_i was obtained from the average of all squared displacements x_{ik} such that
838

839
$$\bar{x}_i = \frac{1}{n_i} \sum_{k=1}^{n_i} x_{ik} \quad (1)$$

840 and

841
$$n_i = N - i + 1 \quad (2)$$

842 where n_i is the number of overlapping time intervals of duration t_i and N the total number of time
843 intervals for the experiment. Mathematically, the persistent random walk model can be written as

844
$$MSD(t) = n_d S^2 P [t - P (1 - e^{-\frac{t}{P}})] \quad (3)$$

845 where S is the migration speed and P is the persistence time. The motility coefficient is given as

846
$$\mu = S^2 P \quad (4)$$

847 where n_d is the dimensionality of the random walk (in this case $n_d=3$). We fitted the PRWM in 3D
848 to obtain estimates of speed, persistence time and motility of each cell track by non-linear
849 regression.

850 **Statistical Analysis:** Statistical analysis was done in GraphPad Prism or in R. For testing null
851 hypothesis between two groups, either Student's t tests and or the non-parametric Mann-Whitney
852 U tests were used, depending on the number and distribution of data points. Likewise, for testing
853 null hypotheses among 3 or more groups, ANOVA or non-parametric tests were performed,
854 followed by post-hoc Holm-Sidak's test, correcting for multiple comparisons. Unless otherwise
855 mentioned, data are representative of at least 2 independent experiments.

856

857

858

859

860

861

862

863

864

865

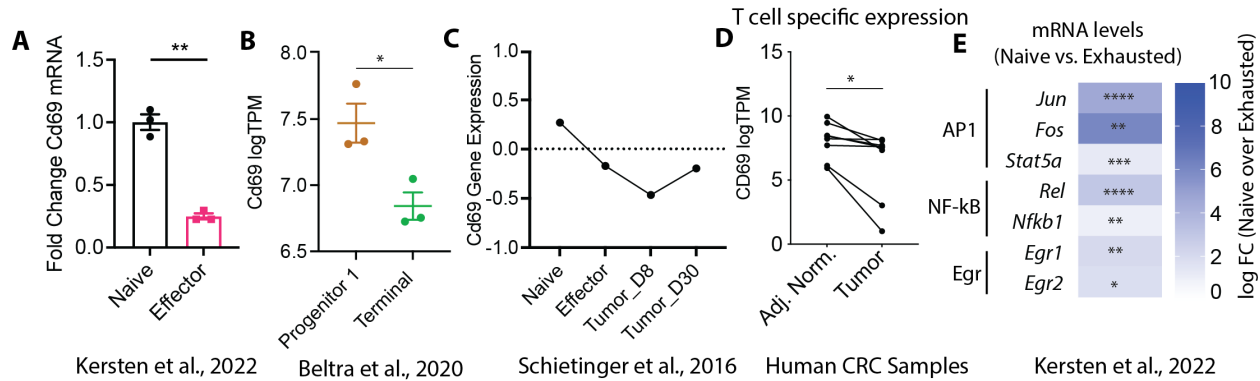
866

867

868

869

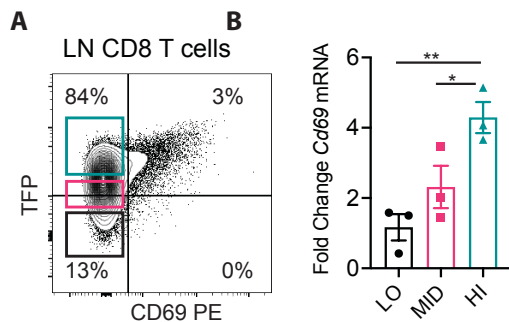
870 **Supplementary Figures:**



871

872 **Fig. S1: Resting Cd69 mRNA decreases with T cell differentiation towards exhaustion.**

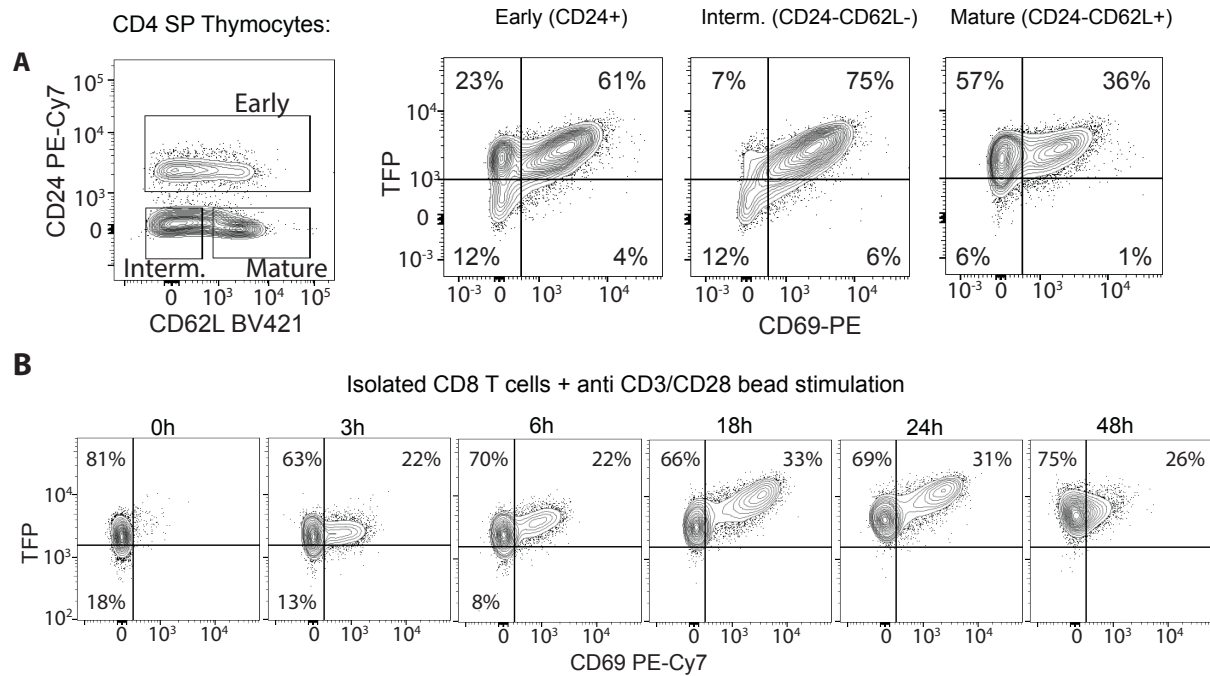
873 Cd69 mRNA expression in (A) Naïve vs. in vitro generated (stimulation with Dynabeads followed
 874 by rest in IL-2 containing media) effector CD8 T cells from published RNASeq data(14); (B)
 875 Progenitor 1 and Terminally exhausted T cell subsets from published data (7), (C) among Naïve,
 876 Effector, D8 tumor and D30 tumor infiltrating T cells from other published data (5), (D) in
 877 conventional T cells sorted from tumor and adjacent normal regions of human colorectal cancer
 878 patients; (E) depressed mRNA expression of factors associated with the Cd69 transcription in
 879 Naïve vs. Exhausted CD8 T cells from previous work (14) (symbols indicate FDR adjusted p-
 880 values). Plots show mean +/- SEM (A, B) p-values obtained by unpaired (A, B) and paired
 881 Student's t test (D).



882

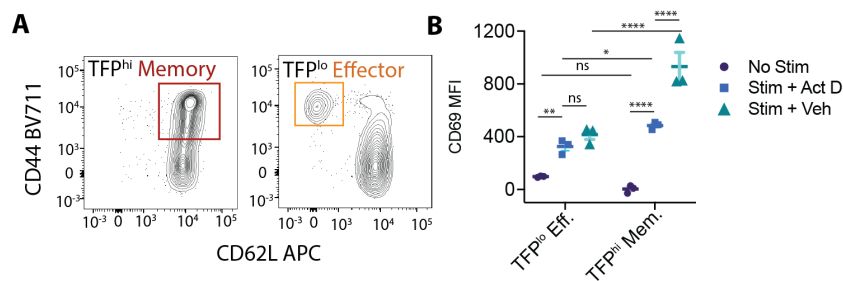
883 **Fig. S2: Cd69-TFP reporter reads out Cd69 transcription.** (A) TFP vs. CD69 in homeostatic

884 lymph node (LN) CD8 T cells with percentage of cells in each quadrant and (B) corresponding
 885 Cd69 mRNA by qPCR from color-coded sorted subpopulations.



886

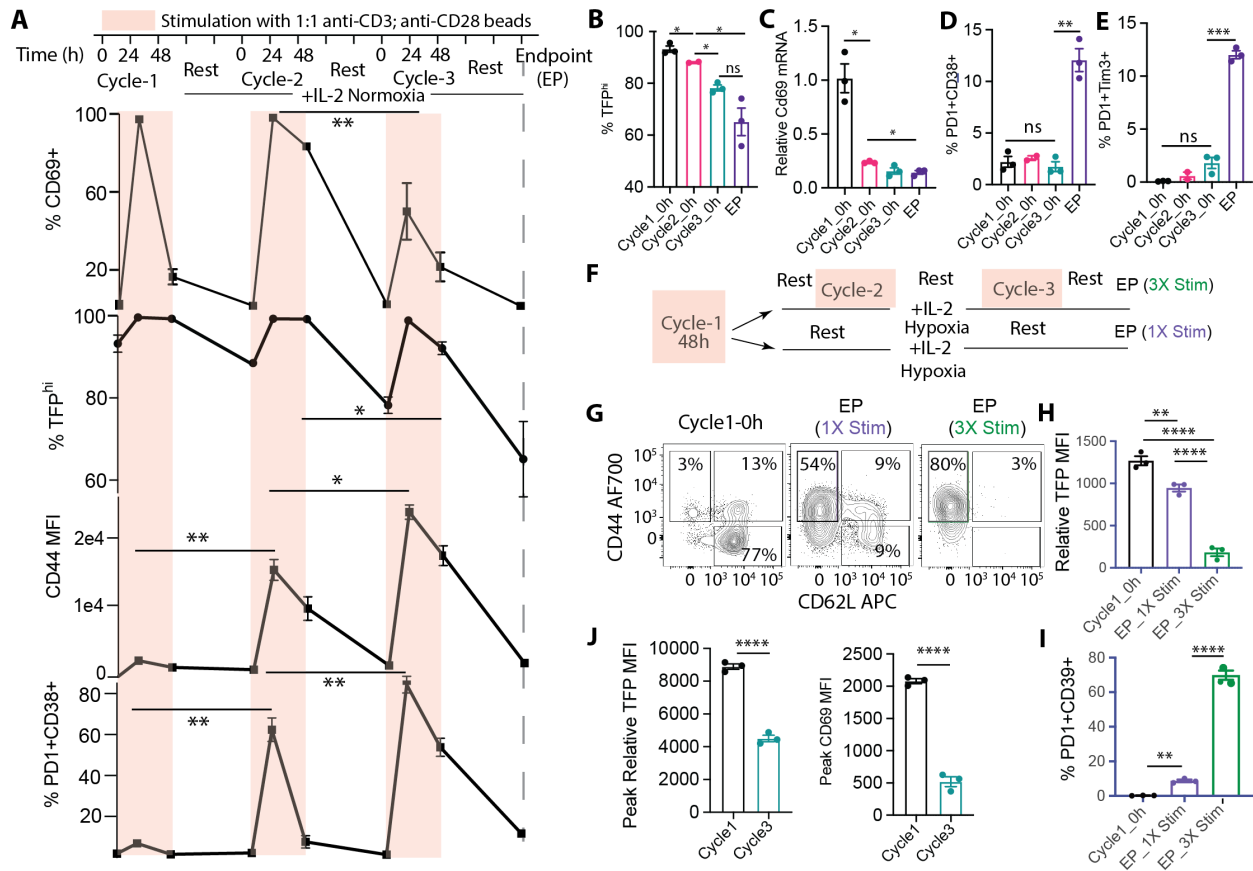
887 **Fig. S3: TFP is upregulated along with CD69 in known contexts of TCR stimulation. (A)**
 888 Representative flow cytometry plot of CD62L and CD24 expression in CD4+CD8- (CD4 single
 889 positive or SP) thymocytes to demarcate early, intermediate (interm.) and mature subsets with
 890 corresponding plots of TFP vs. CD69 in these subsets with varying degree of maturity during
 891 positive selection; **(B)** Representative flow cytometry plots of TFP vs. CD69 of isolated CD8 T
 892 cells from a naïve reporter mouse at different time points post stimulation with α CD3+ α CD28
 893 Dynabeads;



894

895 **Fig. S4: Sensitivity to current stimulation is dependent on initial TFP level. (A)** Typical
 896 phenotypic profile shown by flow cytometry plots of CD44 vs. CD62L from TFP^{lo} (bottom 20%)
 897 and TFP^{hi} (top 20%) splenic CD8 T cells, sorted TFP^{lo} Effector and TFP^{hi} Memory cells are shown
 898 by the corresponding color-coded gates matched with Fig. 1E; **(B)** CD69 MFI of the same sorted
 899 cells without stimulation (No Stim), 3h α CD3+ α CD28 stimulation + DMSO (3h Stim + Vehicle) or
 900 5 μ g/mL Actinomycin D (3h Stim + Act.D); (data representative of one out of at least 2 independent

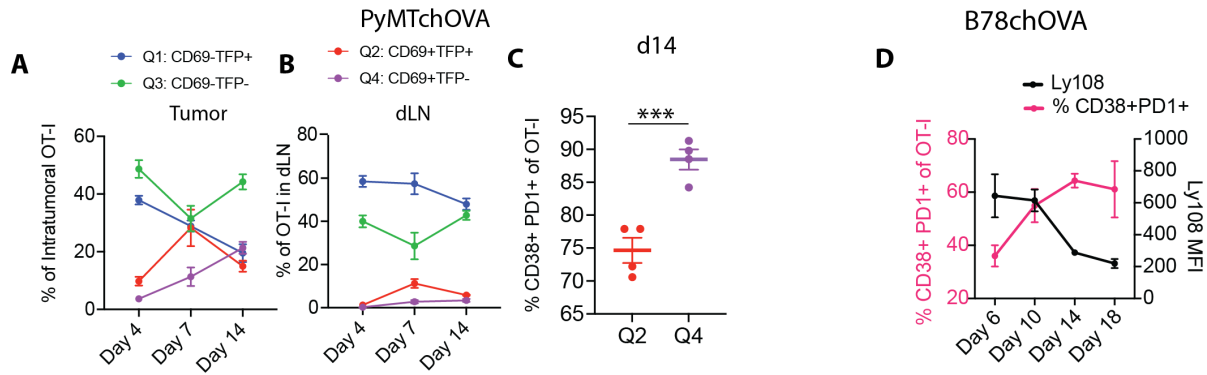
901 experiments, each with 3 mice, bar graphs show mean +/- SEM, null hypothesis testing by
 902 unpaired t test, adjusted for multiple comparisons).



903

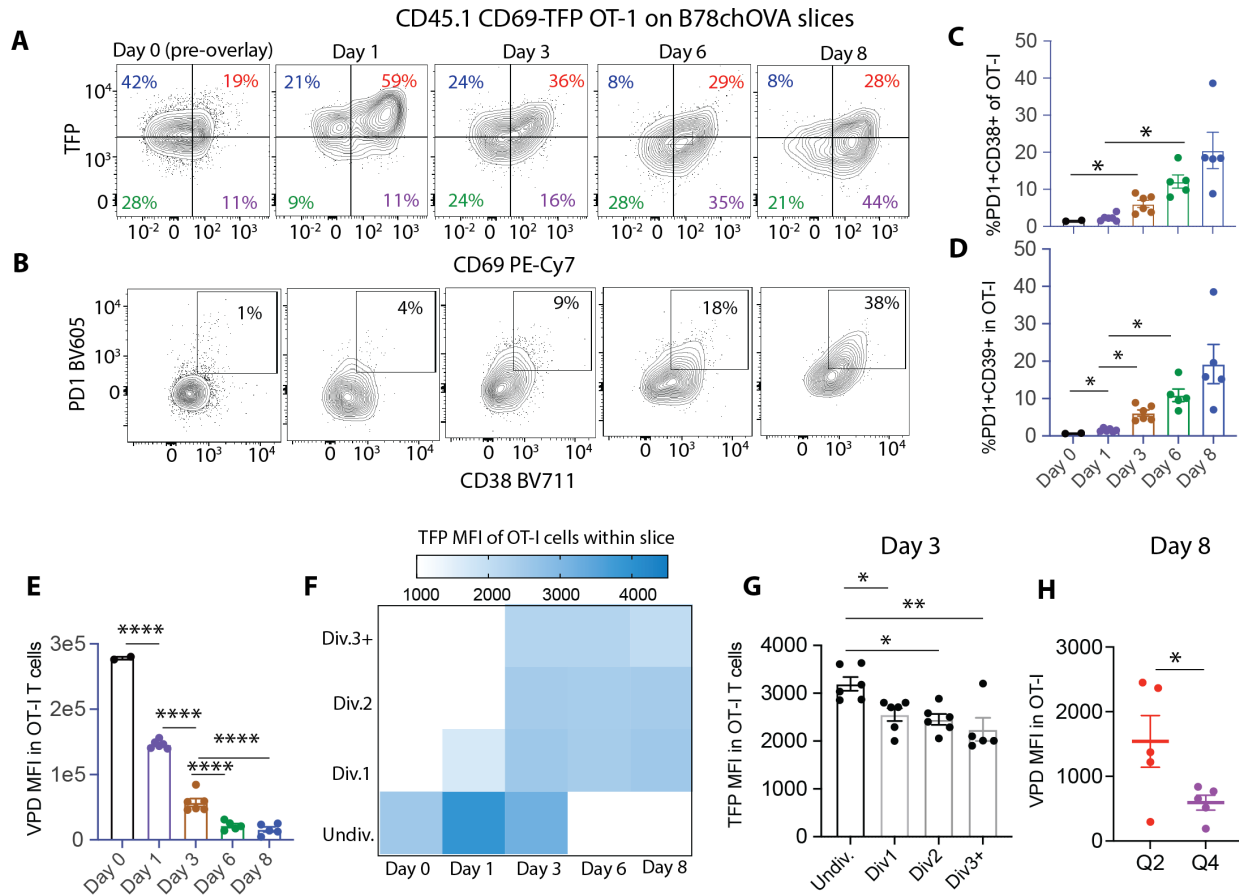
904 **Fig. S5: Repeated TCR stimulation drives down TFP with acquisition of exhaustion markers**

905 **(A)** %CD69+, %TFP^{hi}, CD44 MFI, %PD1⁺CD38⁺ of freshly isolated CD8 T cells through
 906 successive cycles of 48h stimulation and 72h resting in ambient oxygen (normoxia) + IL-2;
 907 **(B)** %TFP^{hi}, **(C)** *Cd69* mRNA by qPCR and **(D)** %PD1⁺CD38⁺, **(E)** %PD1⁺Tim-3⁺ at the beginning
 908 of cycles 1, 2, 3 and endpoint (EP); **(F)** experimental schematic showing 1X Stim vs. 3X Stim
 909 conditions to parse the role of stimulation vs. IL-2 alone; **(G)** flow cytometry plots showing
 910 representative CD44 vs. CD62L profiles of CD8 T cells at the timepoints and conditions indicated;
 911 for the same experiment, **(H)** TFP (relative to WT control), **(I)** %PD1⁺CD39⁺ of CD8 T cells at the
 912 starting point (Cycle1_0h) and at endpoint (EP) either with 1X Stim followed by prolonged rest or
 913 3X stim; **(J)** Peak Relative TFP and CD69 MFI between Cycle 1 and Cycle 3 in normoxia; (bar
 914 graphs represent mean +/- SEM; null hypothesis testing by ANOVA followed by post-hoc Holm-
 915 Šídák test; data representative of 2 independent experiments, each with 3 mice and technical
 916 duplicates/biological replicate at every assay point).



917

918 **Fig. S6: Q4, as opposed to Q2 phenotype dominates terminally exhausted OT-I in tumors**
 919 **(A)** TFP:CD69 quadrant distribution of OT-I T cells from a PyMTchOVA tumor or its corresponding
 920 **(B)** dLN at different time points post injection into tumor-bearing mice; **(C)** %CD38⁺PD1⁺ terminally
 921 exhausted cells among activated d14 intratumoral OT-I belonging to TFP^{hi} Q2 and TFP^{lo} Q4 from
 922 PyMTchOVA tumors; **(D)** %CD38+PD1+ and Ly108 profiles over time (d6-d18) for all intratumoral
 923 OT-I in B78chOVA. Null hypothesis testing by paired t test, bar graphs represent mean +/- SEM;
 924 data representative of 2 independent experiments, each with 2-3 mice for PyMTchOVA (each
 925 PyMTchOVA mice produced more than one tumor) and >=3 mice for B78chOVA per timepoint.

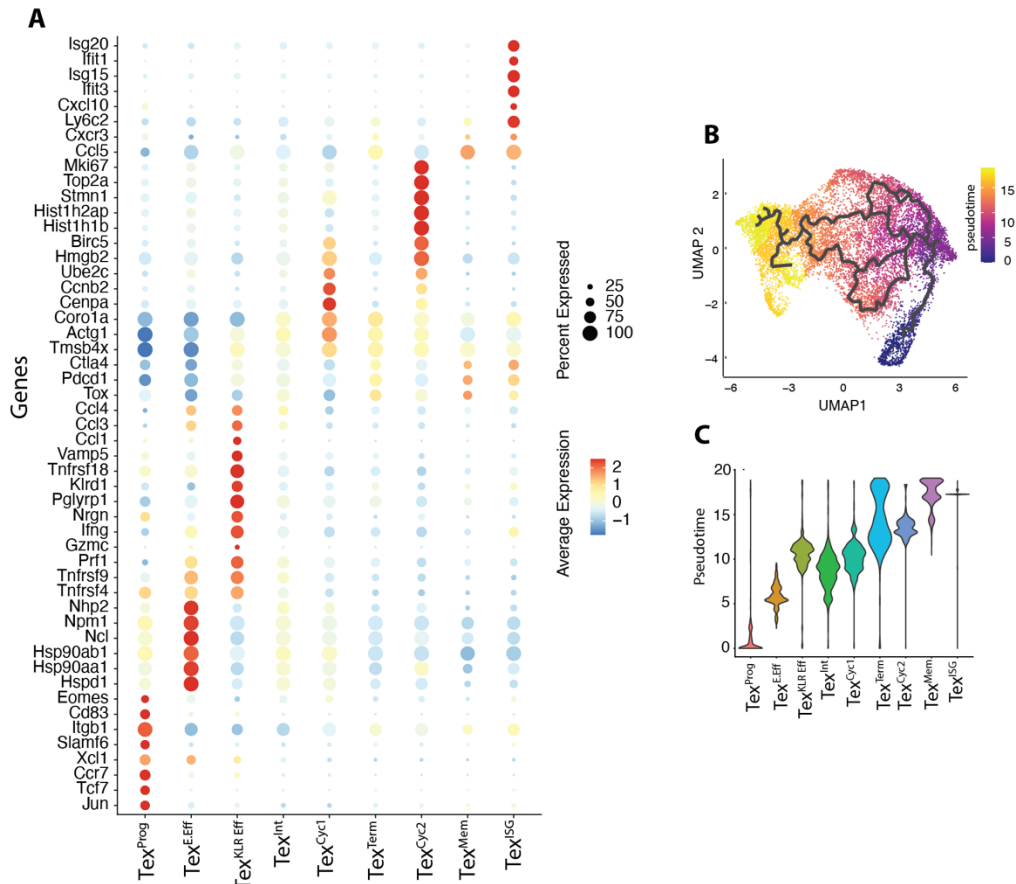


926

927 **Fig. S7: Ex vivo tumor slice overlay culture mimics CD69:TFP dynamics in vivo (A)**
 928 Representative flow cytometry plots of **(E)** TFP vs. CD69 and **(F)** PD1 vs. CD38 expression in
 929 slice-internal OT-I T cell from Day1-Day8, compared to Day0 (pre-overlay); **(B)** %PD1+CD38+,
 930 **(C)** %PD1+CD39+ and **(E)** Violet proliferation dye (VPD) MFI of Day 0 pre-overlay and slice-
 931 internal OT-I T cells at different time points after slice overlay (Day1-Day8); **(F)** heatmap of
 932 average TFP MFI of OT-I CD8 T cells at Day 0 pre-overlay and derived from slice culture from
 933 Day 1-Day 8 grouped by estimated number of divisions (≥ 3 , 2, 1, or divided) and **(G)**
 934 corresponding bar graph showing this quantification for Day 3; **(H)** VPD MFI of slice-internal OT-
 935 ls from Q2 and Q4 at Day8; Bar graphs and line plots show mean \pm SEM, null hypothesis testing
 936 by ANOVA and post hoc Holm-Šídák test, or paired t test in H; data are representative of 2
 937 independent experiments, each 5-6 slices/time point for each slice experiment and Day 0 pre-
 938 overlay samples in duplicate; TFP gated on WT controls CD8 T cells.

939

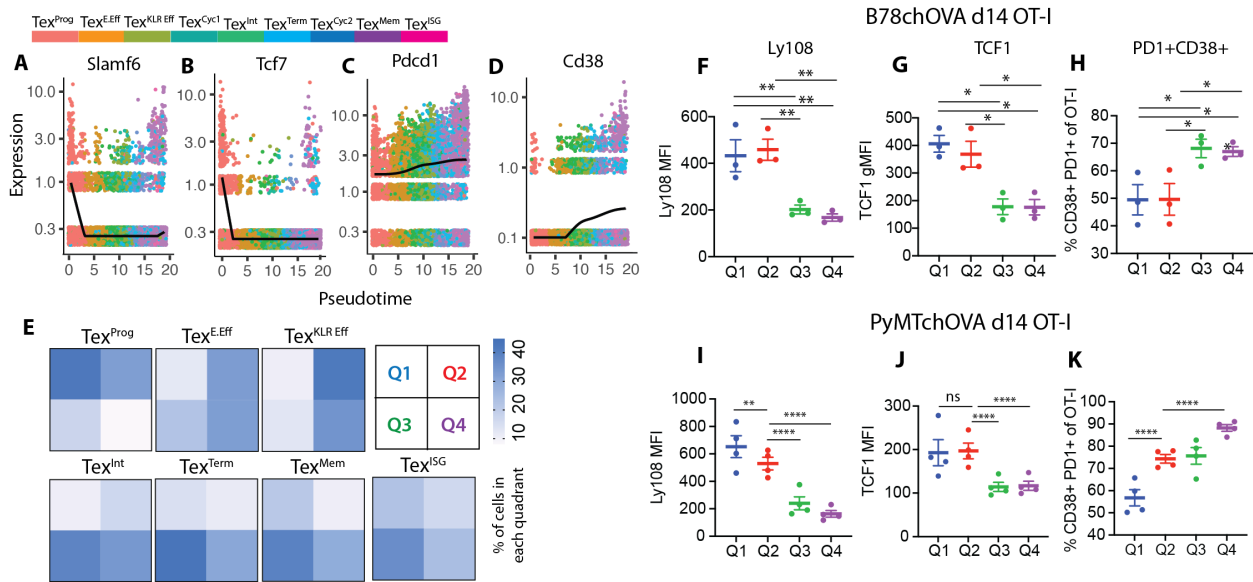
940



941

942 **Fig. S8: Gene expression based clustering of intratumoral OT-Is (A)** Dotplot representation
 943 of differentially expressed and canonical T_{EX}-associated genes across the computationally
 944 derived cell clusters from the scSeq of intratumoral Cd69-TFP:OT-I CD8 T cells at d12 post
 945 injection into B78chOVA tumor-bearing mice; **(B)** UMAP representation of the scSeq data color-
 946 coded by pseudotime derived from Monocle3 trajectory analysis; **(C)** Pseudotime spread of each
 947 cluster.

948



949

950 **Fig. S9: Progenitor, intermediate and terminally exhausted CD8 T cells distribute distinctly**

951 **among CD69:TFP quadrants (A-D)** expression of select genes plotted against pseudotime and

952 color-coded by clusters; best-fitting spline (degrees of freedom=5) to the gene expression pattern

953 overlaid in black, random vertical jitter added to the plot for better visualization; **(E)** heatmaps of

954 percentage of cells by CD69:TFP quadrants Q1-Q4; flow cytometric analysis of select markers

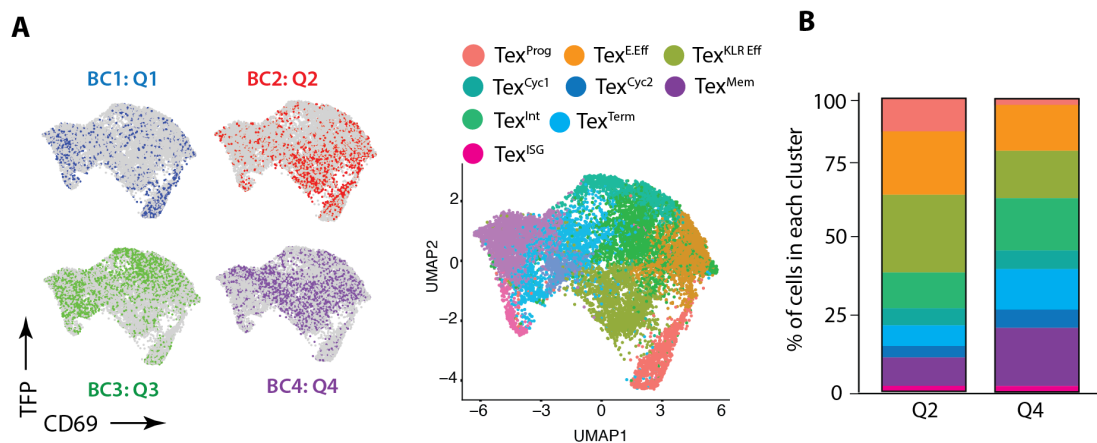
955 from OT-I T cells isolated from **(F-H)** B78chOVA or **(I-K)** PyMTchOVA tumors 14 days post T cell

956 injection grouped by quadrants; (data are mean +/- SEM, representative of >=2 independent

957 experiments with 3-5 mice per experiment, null hypothesis testing by paired RM ANOVA with

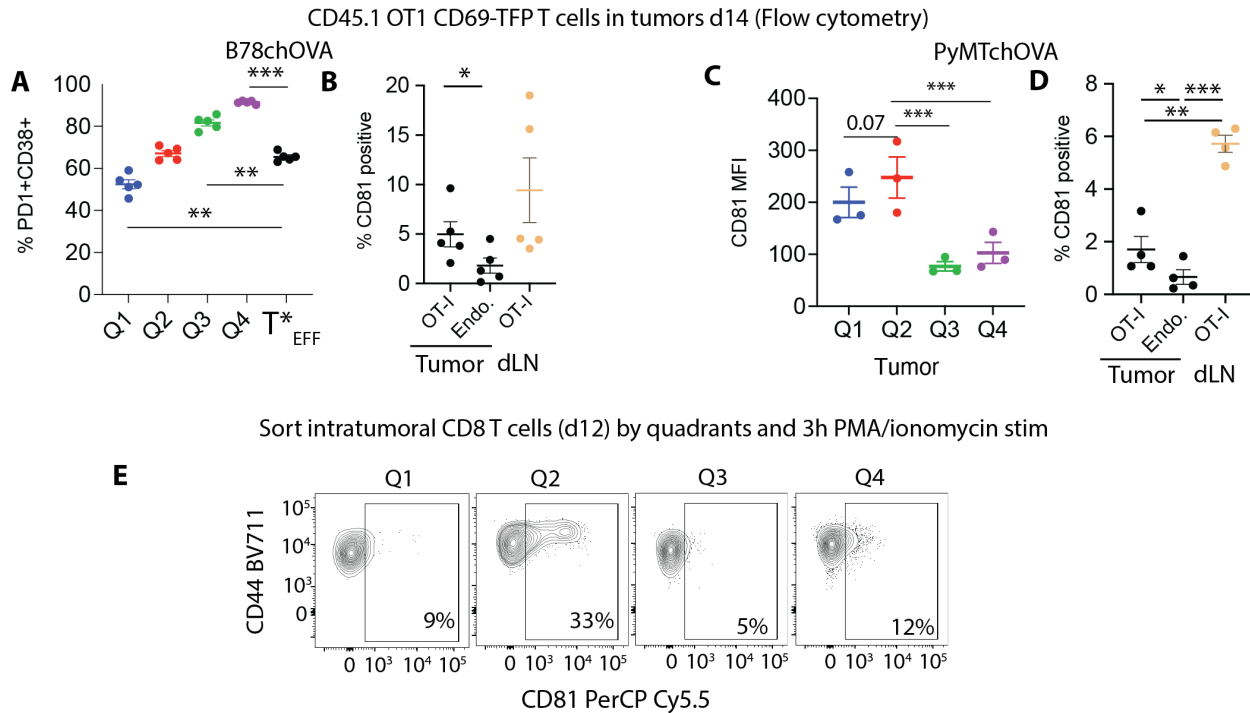
958 post-hoc paired t-tests).

959



960

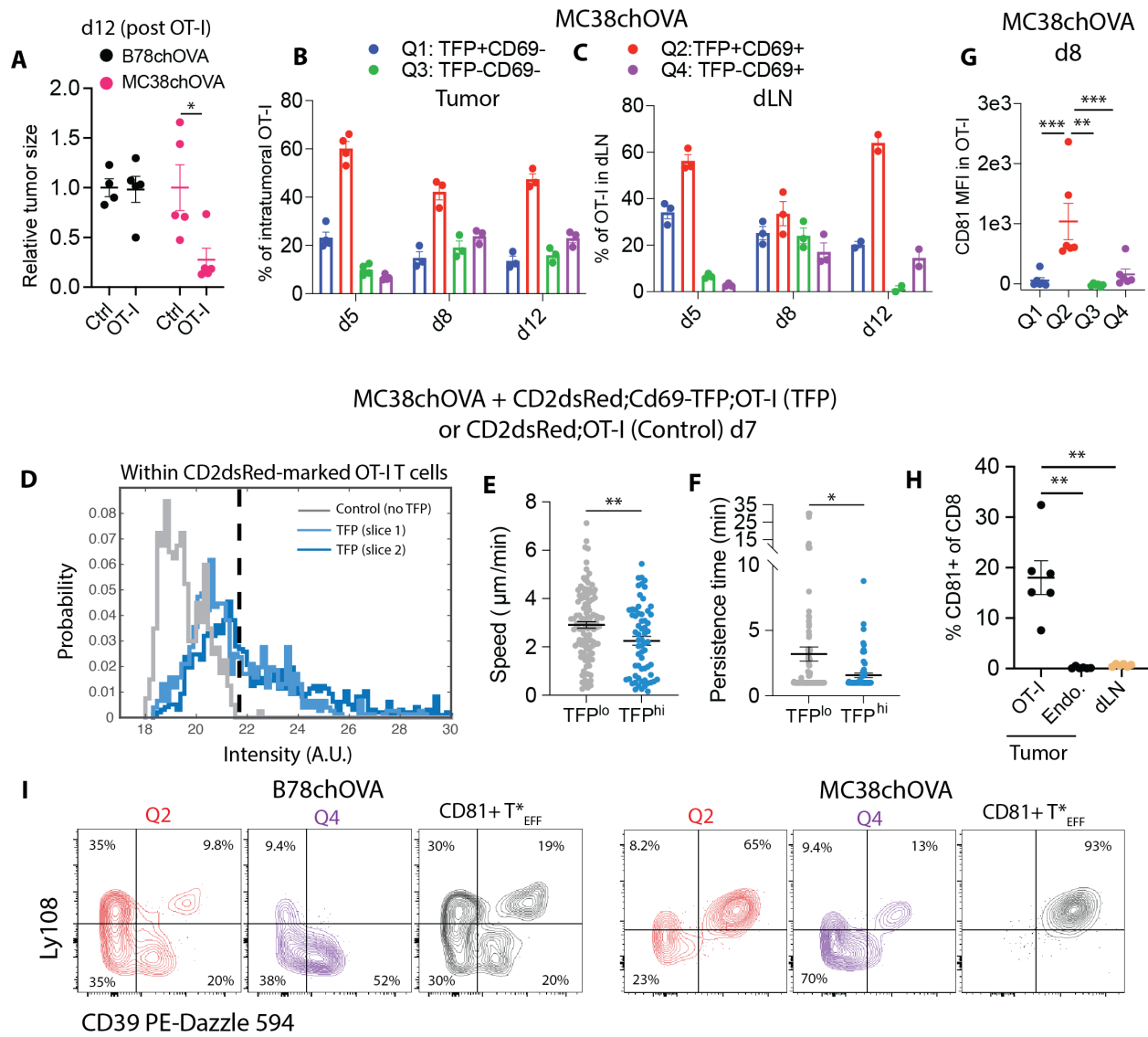
961 **Fig. S10:Q2 is enriched in effectors but not devoid of terminally differentiated T cells. (A)**
 962 Overlay of each CD69:TFP quadrant in the UMAP space with the corresponding clusters shown
 963 side-by-side; **(B)** Stacked bar plot showing the distribution of cells in the computationally-defined
 964 clusters among all Q2 and Q4 cells.



965

966 **Fig. S11: CD81 marks a rare subset of cells in Q2 (A)** %PD1+CD38+ of d14 intratumoral OT-I
 967 T cells in B78chOVA tumors grouped by quadrants and with a subgating to show CD81+ Q2
 968 (T^*_{EFF}) cells; **(B)** % CD81+ among d14 intratumoral OT-I, endogenous T cells and OT-I T cells in
 969 the dLN of mice bearing B78chOVA tumors **(C)** CD81 expression in d14 intratumoral OT-I T cells
 970 in PyMTchOVA tumors grouped by quadrants and **(D)** % CD81+ among d14 intratumoral OT-I,
 971 endogenous T cells and OT-I T cells in the dLN of mice bearing PyMTchOVA tumors (data
 972 representative of 2 independent experiments with 3-4 tumors per experiment; **(E)** CD81
 973 expression among the quadrant-sorted populations; Bar graphs show mean +/- SEM; null
 974 hypothesis testing by RM ANOVA and post hoc paired t test (A, C) and by ANOVA and post hoc
 975 Holm-Šídák test (B, D).

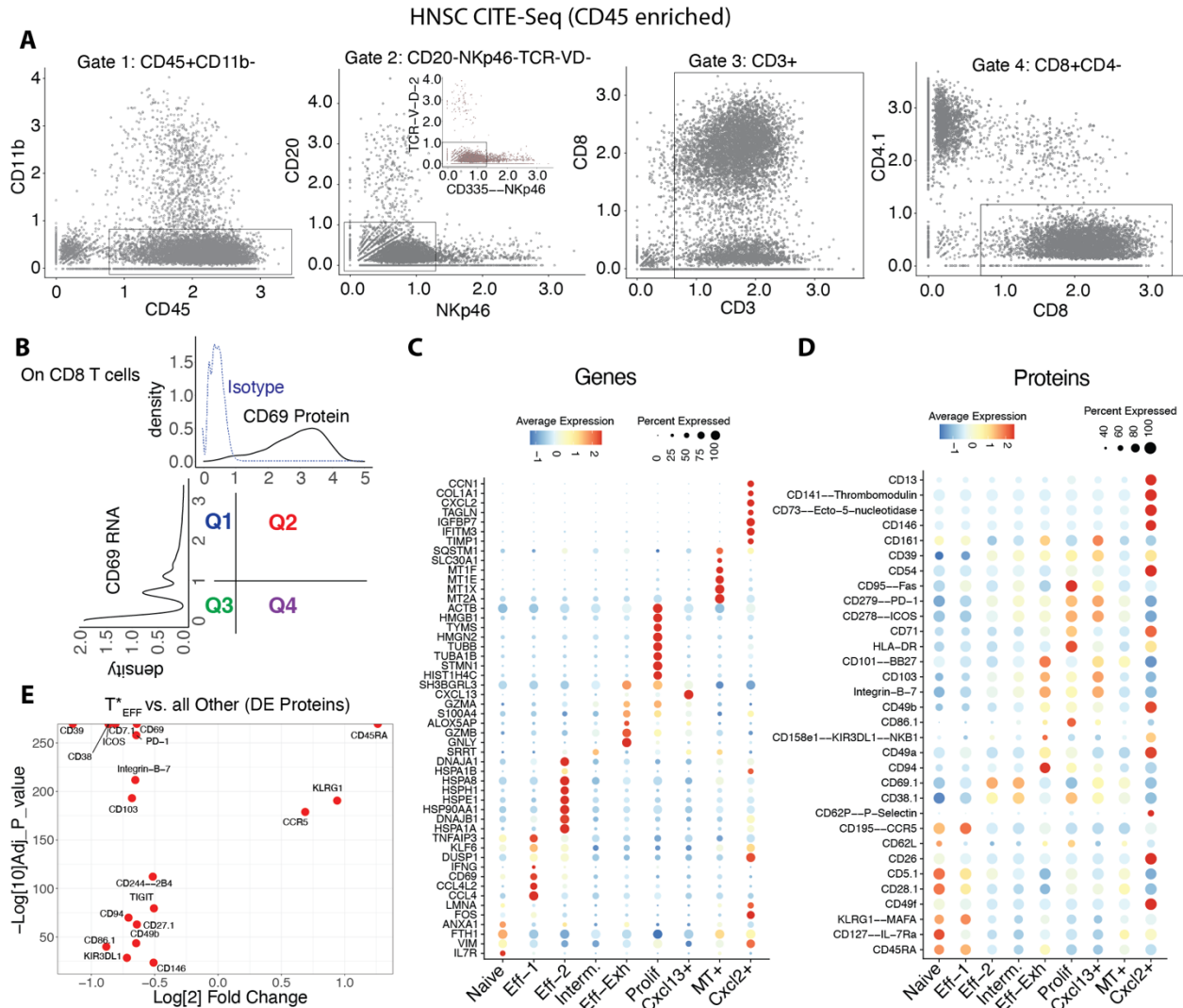
976



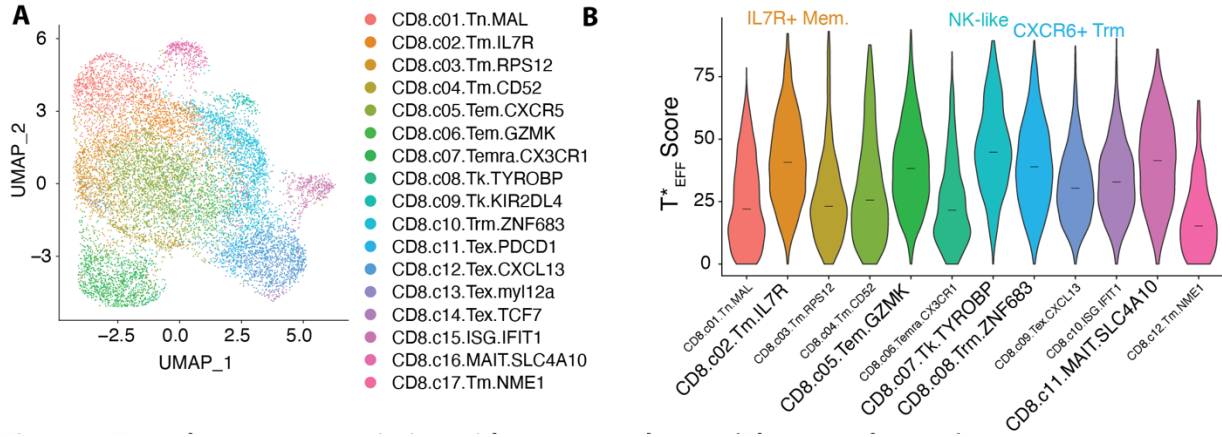
977

978 **Fig. S12: Features of Q2 OT-I T cells in MC38chOVA tumors.** (A) B78chOVA and MC38chOVA
 979 tumor sizes relative to the mean of the Ctrl group d12 post adoptive transfer of Cd69-
 980 TFP;CD45.1;OT-I T cells; in Bar graphs showing TFP:CD69 quadrant distribution among OT-I
 981 CD8 T cells in (B) tumors and (C) tdLN at d5, d8, d12 post T cell injection into MC38chOVA tumor-
 982 bearing mice corresponding dLNs (n=3-4 mice per group respectively); (D) Representative
 983 histograms of channel intensity within OT-I T cells in live tumor slices to find TFP^{hi} cells using
 984 CD2dsRed and CD2dsRed;Cd69-TFP OT-Is; (E) Speed and (F) Persistence of TFP^{hi} vs. TFP^{lo}
 985 intratumoral OT-Is d8 post adoptive transfer within live MC38chOVA tumor slices; (G) CD81
 986 expression in d8 intratumoral OT-I T cells grouped by quadrants; (H) % CD81+ among d8
 987 intratumoral OT-I, endogenous T cells and OT-I T cells in the dLN of mice bearing B78chOVA
 988 tumors; (I) Ly108 vs. CD39 expression profiles in d12 (B78chOVA) and d8 (MC38chOVA)

989 intratumoral OT-Ts, separated by Q2, Q4 and CD81+ T*_{EFF} subsets; bar graphs show mean +/-
 990 SEM, null hypothesis testing by unpaired t test (A), Mann-Whitney U test (E, F), paired RM
 991 ANOVA with post-hoc paired t-tests.



992
 993 **Fig. S13: CITE-Seq of HNSC tumor sample allows mapping of quadrants onto cell**
 994 **phenotypes (A)** Gating scheme of CD45-enriched HNSC CITE-Seq data using protein markers
 995 to isolate a pure CD8 population; **(B)** Gating of the CD8 population into CD69 Protein: CD69 RNA
 996 quadrants; **(C)** DEGs and **(D)** DE Proteins for the computationally derived subsets obtained
 997 through multimodal clustering using both protein and RNA; **(E)** Volcano plot showing DE Proteins
 998 in the T*_{EFF} (Q2 ∩ Eff-1) vs. all other CD8 T cells pre-filtered by a p-value <0.01 and average
 999 abs(log₂ fold change) >0.5;



1000

1001 **Fig. S14: T*_{EFF} phenotype association with CD8 metaclusters. (A)** UMAP representation of
1002 computationally-derived subsets among CD8 T cells in a pan-cancer T cell atlas(30) and **(B)**
1003 Violin plot showing the T*_{EFF} signature score across those subsets – black line denotes median.

1004

1005